Research Article

Robust H_∞ Control for Path Tracking of Network-Based Autonomous Vehicles

Changfang Chen [ID], Minglei Shu, Yinglong Wang, and Ruixia Liu

Shandong Computer Science Center (National Supercomputer Center in Jinan),
Shandong Provincial Key Laboratory of Computer Networks, Qilu University of Technology (Shandong Academy of Sciences),
Jinan 250014, China

Correspondence should be addressed to Changfang Chen; chenchangfang012@163.com

This paper investigates the robust H_∞ path-tracking control problem of network-based autonomous vehicles (AVs) with delay and packet dropout. Generally, both network-induced delay and packet dropout bring negative effects on the system stability and performance. A robust H_∞ control scheme is proposed to realize the desired path tracking and lateral stability. The closed-loop system is asymptotically stable with the prescribed H_∞ disturbance attention level if there exist some matrices satisfying certain linear matrix inequality (LMI) conditions. Furthermore, the proposed controller is robust to the parameter uncertainties and external disturbances. Simulation results are presented to verify the effectiveness of the proposed control scheme.

1. Introduction

With the advantages of improved security, better road utilization, and greatly reduced mobility costs, autonomous vehicles (AVs) offer the possibility of fundamentally changing the conventional transportation system [1]. One of the rudimentary control issues for AVs is the path-tracking control. The objective is to control the vehicle to track the predefined desired path with zero steady-state tracking errors, including lateral offset and heading error [2, 3]. Generally, to reduce the traffic accidents, the path-tracking errors (especially the lateral offset) must be guaranteed in reasonable and safe regions, either in mitigative or extreme driving conditions.

Several control strategies are proposed for the traditional vehicle stability and handling control, for example, robust H_∞ control [4, 5], model predictive control methods [6, 7], and Lyapunov-based control approaches [8–10]. In [11], a robust linear quadratic regulator-based H_∞ controller is proposed to improve stability and handling of four-wheel independently actuated electric vehicles with the norm-bounded uncertainties. A robust

gain-scheduled H_∞ controller is developed for lateral stability control of electric vehicles via linear parameter-varying technique [12], and the quadratic D-stability is applied to improve the transient response of the closed-loop system. In [13], a distributed robust H_∞ control method is presented for multivehicle systems to balance the performance of robust stability, tracking performance, and string stability of a platoon. In [14], a hierarchical adaptive path-tracking controller is designed for an autonomous vehicle to track a reference path in the presence of uncertainties in both tire-road condition and external disturbance. In [15], the authors address the problem of position trajectory tracking and path-following control for underactuated autonomous vehicles in the presence of possibly large modeling parametric uncertainty. In [16], a composite nonlinear feedback control is investigated for path-tracking control of four-wheel independently actuated AVs considering the tire force saturations.

All of these aforementioned control methods consider the autonomous vehicle as a centralized control system. However, with the development of in-vehicle networks, the autonomous vehicle is actually a networked control system

rather than a centralized control system. The control and measurement signals from controllers and sensors are exchanged through communication network, which imposes the effects of network-induced delays and packet dropout on the control loop due to the bandwidth limitation. The unavoidable delay and packet dropout during the signal transmissions will probably degrade the control effect and deteriorate the system stability [17–19]. Thus, this paper aims to solve the path-tracking control problem for AVs in presence of the delay and packet dropout. And we can obtain the useful inspirations from some well-studied theoretical results. In [20], new results on stability and H_∞ performance are obtained for time-delay systems with two successive delay components by exploiting a new Lyapunov–Krasovskii functional. In [21], the H_∞ fault detection problem is addressed for time-delay delta operator systems with random two-channel packet losses and limited communication. The sufficient conditions for the asymptotical stability and H_∞ performance of the delta operator systems are provided by the Lyapunov functional technique. In order to save the communication resources with limited bandwidth, the event-triggered schemes are developed for networked control systems [22–24], and the stability and H_∞ performance for the closed-loop system are obtained in terms of a group of LMIs. In [25–27], the tracking performance of networked control systems under the packet dropouts and channel noise is investigated. It is shown that the optimal tracking performance is related to the nonminimum phase zeros, unstable poles of the given plant, and the packet dropout probability. In [28], a novel characteristic equation-based small-signal modeling approach is proposed for converter-dominated ac microgrids to assess the system low-frequency stability. The distributed energy management algorithms are presented for the energy system formed by many energy bodies, and the main purpose is to maximize the resource allocation while meeting the coupled matrix constraint and the system operation constraints [29–31].

The robust H_∞ control synthesis problem is investigated in the paper to achieve the desired path tracking for network-based autonomous vehicles with delay and packet dropout, parameter uncertainties, and external disturbances. The main contributions of the paper are addressed as follows. Different from the traditional vehicle stability and handling control, the networked-induced delay and packet dropout are considered in the control design, and the yaw rate and the sideslip angle are regulated simultaneously to improve the vehicle stability. The existence conditions of the robust H_∞ path-tracking controller are obtained in terms of LMIs, and the closed-loop system is asymptotically stable with a guaranteed H_∞ performance. In addition, the uncertainty effects of the tire cornering stiffness and external disturbance are considered to enhance the robustness of the proposed control scheme.

The paper is organized as follows. In Section 2, the autonomous vehicle model and path-tracking model are described, where the parametric uncertainties and delay and packet dropout are introduced. In Section 3, the problem of robust H_∞ path-tracking control design for network-based autonomous vehicles is solved and the corresponding LMI conditions for the existence of desired state-feedback controllers are presented. The simulation results are given in Section 4. Finally, the paper concludes in Section 5.

Notation. The notations used in the paper are summarized as follows. The superscripts T and -1 denote matrix transposition and matrix inverse, respectively. The notation $Q > 0$ (≥ 0) means that Q is symmetric and positive definite (semidefinite). If the dimensions of matrices are not explicitly stated, it is assumed to be compatible for algebraic operations. In symmetric block matrices, the notation $*$ represents a term that is induced by symmetry. And notation diag$\{\cdots\}$ stands for a block-diagonal matrix.

2. System Modeling

The dynamics of the autonomous vehicle is shown in Figure 1, which has the following lateral and yaw degrees of freedom (DOF). Assuming that the front-wheel steering angle is small, the dynamic equations can be described as

$$
\begin{aligned}
\dot{\beta} &= \frac{1}{mv_x}\left(F_{yf} + F_{yr}\right) - \gamma + w_1, \\
\dot{\gamma} &= \frac{1}{Iz}\left(l_f F_{yf} - l_r F_{yr}\right) + w_2,
\end{aligned}
\tag{1}
$$

where v_x is the longitudinal velocity of center of gravity (CG), β is the vehicle sideslip angle, and γ is the yaw rate. w_1 and w_2 model the external disturbance. m and I_z are the mass of vehicle and the inertia about the z-axis, respectively. l_f and l_r denote the distances from CG to the front and rear axles.

The lateral tire forces of the front and rear wheels can be described as

$$
\begin{aligned}
F_{yf} &= 2C_f \alpha_f, \\
F_{yr} &= -2C_r \alpha_r,
\end{aligned}
\tag{2}
$$

where the proportionality constants C_f and C_r are the front and rear cornering stiffness and α_f and α_r are the tire slip angles of the front and rear wheels. Supposing the vehicle sideslip angle is sufficiently small, it follows that $v_y = v_x \beta$. And α_f and α_r can be calculated as

$$
\begin{aligned}
\alpha_f &= \delta_f - \frac{v_y + l_f \gamma}{v_x}, \\
\alpha_r &= \frac{v_y - l_r \gamma}{v_x},
\end{aligned}
\tag{3}
$$

where δ_f is the wheel steering angle used for the control scheme. From (1)–(3), the vehicle dynamics can be expressed as follows:

$$
\begin{aligned}
\dot{\beta} &= a_{11}\beta + a_{12}\gamma + b_1 \delta_f + w_1, \\
\dot{\gamma} &= a_{21}\beta + a_{22}\gamma + b_2 \delta_f + w_2,
\end{aligned}
\tag{4}
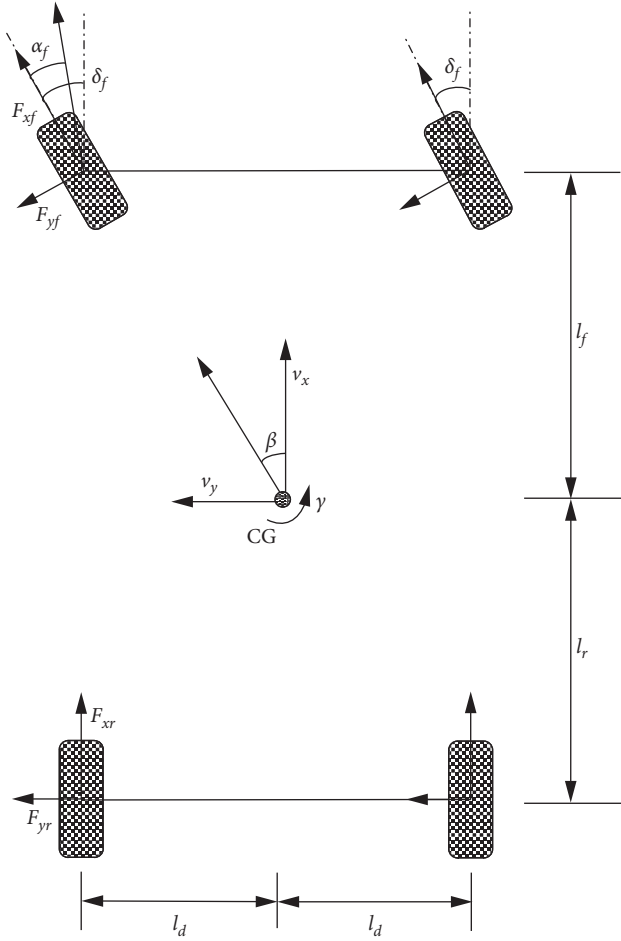$$

Figure 1: Schematic diagram of the vehicle model.

where

$$a_{11} = -\frac{2C_f + 2C_r}{mv_x},$$

$$a_{12} = -1 - \frac{2C_f l_f - 2C_r l_r}{mv_x^2},$$

$$a_{21} = -\frac{2C_f l_f - 2C_r l_r}{I_z},$$

$$a_{22} = -\frac{2C_f l_f^2 + 2C_r l_r^2}{I_z v_x}, \tag{5}$$

$$b_1 = \frac{2C_f}{m},$$

$$b_2 = \frac{2C_f l_f}{I_z}.$$

The path-tracking model of the autonomous vehicle is shown in Figure 2, where y_e is the lateral offset of the vehicle with respect to the lane centerline at a preview distance l_s and ϕ_e is the angle between vehicle longitudinal axis and the

road centerline. The relationship between y, y_e, and ϕ_e can be described as

$$\phi_e = \frac{y_e - y}{l_s}, \tag{6}$$

where l_s is the horizontal distance from the CG to the sensor.

Denote ϕ_d as the yaw angle of the road centerline with respect to the global coordinate frame; then, the vehicle yaw angle can be written as

$$\phi = \phi_e + \phi. \tag{7}$$

To track the reference path of road curvature ρ_{ref} at a longitudinal velocity v_x, the absolute desired yaw rate should be $v_x \rho_{\text{ref}}$, i.e., $\dot{\phi}_d = v_x \rho_{\text{ref}}$. In practice, ρ_{ref} can be measured using a combined GPS/GIS system.

By differentiating (6) and (7), the path-tracking model is given as follows:

$$\dot{\phi}_e = \gamma - v_x \rho_{\text{ref}},$$
$$\dot{y}_e = v_x (\beta + \phi_e) + l_s (\gamma - v_x \rho_{\text{ref}}). \tag{8}$$

Define the state vector $x = [\beta, \gamma, \phi_e, y_e]^T$ and the control input $u(t) = \delta_f$. Combining (4) and (8), the dynamics of the overall system in the state-space form can be denoted by

$$\dot{x}(t) = Ax(t) + Bu(t) + B_w w(t), \tag{9}$$

where

$$A = \begin{bmatrix} -\dfrac{2C_f + 2C_r}{mv_x} & -1 - \dfrac{2C_f l_f - 2C_r l_r}{mv_x^2} & 0 & 0 \\[3mm] -\dfrac{2C_f l_f - 2C_r l_r}{I_z} & -\dfrac{2C_f l_f^2 + 2C_r l_r^2}{I_z v_x} & 0 & 0 \\[3mm] 0 & 1 & 0 & 0 \\[3mm] v_x & l_s & v_x & 0 \end{bmatrix}, \tag{10}$$

$$B = \begin{bmatrix} \dfrac{2C_f}{m} & \dfrac{2C_f l_f}{I_z} & 0 & 0 \end{bmatrix}^T,$$

$$B_w = I,$$

$$w = \begin{bmatrix} w_1 & w_2 & -v_x \rho_{\text{ref}} & -l_s v_x \rho_{\text{ref}} \end{bmatrix}^T.$$

Due to the change of the road conditions, the tire-cornering stiffness is assumed to be time varying, which can be expressed as multiplicative perturbations:

$$C_f = (1 + \kappa_f) C_{f0},$$
$$C_r = (1 + \kappa_r) C_{r0}, \tag{11}$$

where κ_f and κ_r are the time-varying parameters, satisfying $|\kappa_i| \leq 1$, $i = f, r$, and C_{f0} and C_{r0} are the nominal values of C_f and C_r, respectively. Thus, it follows that
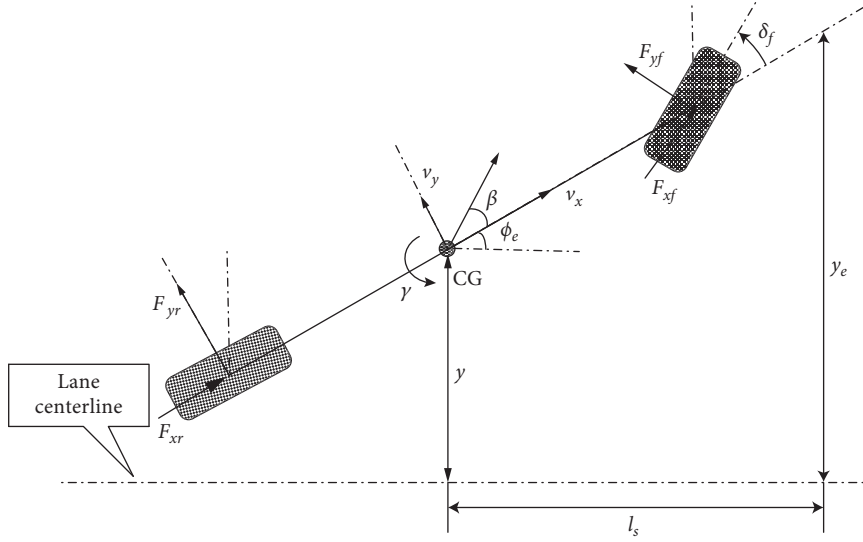
FIGURE 2: Schematic diagram of path-tracking model.

$$A = A_0 + \Delta A,$$
$$B = B_0 + \Delta B,$$
(12)

where A_0 and B_0 are the nominal values of A and B, respectively. ΔA and ΔB are the variations of A and B, and $\Delta A = \kappa_f A_{cf} + \kappa_r A_{cr}$ and $\Delta B = \kappa_f B_{cf}$, where

$$A_0 = \begin{bmatrix} \bar{a}_{11} & \bar{a}_{12} & 0 & 0 \\ \bar{a}_{21} & \bar{a}_{22} & 0 & 0 \\ 0 & 1 & 0 & 0 \\ v_x & l_s & v_x & 0 \end{bmatrix},$$

$$B_0 = \begin{bmatrix} \bar{b}_1 & \bar{b}_2 & 0 & 0 \end{bmatrix}^T,$$

$$A_{cf} = \begin{bmatrix} -\dfrac{2C_{f0}}{mv_x} & -\dfrac{2l_f C_{f0}}{mv_x^2} & 0 & 0 \\ -\dfrac{2l_f C_{f0}}{I_z} & -\dfrac{2l_f^2 C_{f0}}{I_z v_x} & 0 & 0 \\ 0 & 0 & 0 & 0 \\ 0 & 0 & 0 & 0 \end{bmatrix},$$

$$A_{cr} = \begin{bmatrix} -\dfrac{2C_{r0}}{mv_x} & \dfrac{2l_r C_{r0}}{mv_x^2} & 0 & 0 \\ \dfrac{2l_r C_{r0}}{I_z} & -\dfrac{2l_r^2 C_{r0}}{I_z v_x} & 0 & 0 & 0 & 0 \\ 0 & 0 & 0 & 0 \end{bmatrix},$$

$$B_{cf} = \begin{bmatrix} \dfrac{2C_{f0}}{m} & \dfrac{2l_f C_{f0}}{I_z} & 0 & 0 \end{bmatrix}^T,$$

$$\bar{a}_{11} = -\dfrac{2C_{f0} + 2C_{r0}}{mv_x},$$

$$\bar{a}_{12} = -1 - \dfrac{2C_{f0}l_f - 2C_{r0}l_r}{mv_x^2},$$

$$\bar{a}_{21} = -\dfrac{2C_{f0}l_f - 2C_{r0}l_r}{I_z},$$

$$\bar{a}_{22} = -\dfrac{2C_{f0}l_f^2 + 2C_{r0}l_r^2}{I_z v_x},$$

$$\bar{b}_1 = \dfrac{2C_{f0}}{m},$$

$$\bar{b}_2 = \dfrac{2C_{f0}l_f}{I_z}.$$
(13)

To deal with the uncertainties, the parameter matrices can be expressed as

$$\begin{bmatrix} \Delta A & \Delta B \end{bmatrix} = H\Lambda \begin{bmatrix} E_1 & E_2 \end{bmatrix},$$
(14)

where $H = \begin{bmatrix} A_{cf} & A_{cr} & B_{cf} \end{bmatrix}$, Λ is the 9×9 diagonal matrix of the uncertain parameters, and E_1 and E_2 are the 9×4 and 9×1 constant matrices, respectively. For the uniform road conditions of the front and rear wheels, we can suppose $\kappa_f = \kappa_r$ to reduce the possible design conservation. So the path-tracking model can be rewritten as

$$\dot{x}(t) = (A_0 + \Delta A)x(t) + (B_0 + \Delta B)u(t) + B_w w(t).$$
(15)

As the active safety systems become more advanced, much information about the state of the vehicle can be obtained by direct measurement. For example, vehicle sideslip angle, lateral offset, and heading error can be

obtained by GPS, while the yaw rate can be measured by the vehicle on-board inertial measurement unit [32]. However, due to the network congestion or node failure, there unavoidably exist delay and packet dropout in the vehicle control system.

The networked path-tracking control scheme is shown in Figure 3. The whole delay is denoted by $\tau_i = \tau_{ca} + \tau_{sc}$ at each sampling period, where τ_{ca} is the controller-to-actuator delay and τ_{sc} is the sensor-to-controller delay at sampling time t_i. Considering the behavior of the zero-order-hold in the control system, the data packets received by the networked controller are expressed as

$$\begin{cases} \widehat{x}(t_i) = x(t_i), & \text{if } n(i) = 0, \\ \widehat{x}(t_i) = x(t_i - h), & \text{if } n(i) = 1, \\ \widehat{x}(t_i) = x(t_i - mh), & \text{if } n(i) = m, \end{cases} \quad (16)$$

where h denotes the sampling period and $n(i)$ represents the number of the packet dropout at the time t_i. Thus, by lumping network-induced delay and packet dropout together, it can be deduced that

$$\widehat{x}(t_i) = x(t_i - mh - \tau_i). \quad (17)$$

Let $\tau(t) = t - (t_i - mh - \tau_i)$; we can obtain

$$\widehat{x}(t_i) = x(t - \tau(t)). \quad (18)$$

Assuming that the time-varying delay satisfies $0 < \tau(t) \le \tau_{max}$, where τ_{max} is the upper bound of delay. Due to the transmission of the system state to the controller with network-induced delay and packet dropout, the state received by the controller at sampling instant t_i is $\widehat{x}(t_i)$, so by utilizing parallel distributed compensation scheme, the state-feedback controller can be designed as follows:

$$u(t) = K\widehat{x}(t_i), \quad (19)$$

where K is the control gain to be designed.

To finish the path-tracking task of autonomous vehicles, it is needed to control the lateral offset y_e and heading error ϕ_e as small as possible. Besides, the yaw rate γ and sideslip angle β should be well regulated to assure the vehicle lateral stability. Choose the controlled outputs as $z = Cx = [\beta \;\; \gamma \;\; \phi_e \;\; y_e]^T$, and combining (15) and (19), the closed-loop path-tracking vehicle model can be expressed as

$$\begin{aligned} \dot{x}(t) &= (A_0 + \Delta A)x(t) + (B_0 + \Delta B)Kx(t - \tau(t)) + B_w w(t), \\ z(t) &= Cx(t). \end{aligned} \quad (20)$$

The control objective is to design a robust H_∞ path-tracking controller such that the closed-loop controlled system in (20) is asymptotically stable with an H_∞ disturbance attenuation level γ_0, i.e.,

$$\int_0^t z^T(t)z(t)\mathrm{d}t \le \gamma_0^2 \int_0^t w^T(t)w(t)\mathrm{d}t. \quad (21)$$
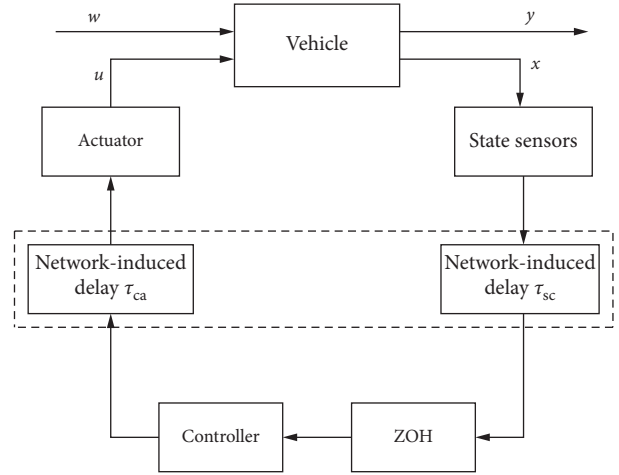

Figure 3: Schematic diagram of the networked path-tracking control system.

3. Controller Design

This section is devoted to solve the problem of robust H_∞ path-tracking control of autonomous vehicles with network-induced delay and packet dropout. We study the conditions under which the closed-loop path-tracking control system is asymptotically stable with the prescribed H_∞ disturbance attention performance. Before proceeding further, the following lemmas are introduced.

Lemma 1. *Given matrices Σ_1, Σ_2, and Σ_3 of appropriate dimensions, $\Sigma_1 = \Sigma_1^T$, and W satisfies $WW^T < I$, then the following condition:*

$$\Sigma_1 + \Sigma_2 W \Sigma_3 + \Sigma_3^T W^T \Sigma_2^T < 0, \quad (22)$$

holds if and only if there exists a positive scalar $\epsilon > 0$ such that

$$\Sigma_1 + \epsilon \Sigma_2 \Sigma_2^T + \epsilon^{-1} \Sigma_3^T \Sigma_3 < 0. \quad (23)$$

Lemma 2. *If there exist matrices P and $W > 0$, then the following conditions are equivalent:*

$$\begin{aligned} &(1)\,(P - W)^T P^{-1}(P - W) \ge 0, \\ &(2) -WP^{-1}W \le P - 2W. \end{aligned} \quad (24)$$

Theorem 1. *Given positive constants γ_0, τ_{max}, and control gain matrix K, closed-loop system (20) is asymptotically stable with an H_∞ disturbance attention level γ_0 if there exist matrices $P > 0$, $Q > 0$, $R > 0$, general matrices N_i, $i = 1, \ldots, 4$, and a scalar $\epsilon > 0$ satisfying*

$$\begin{bmatrix} \overline{\Pi}_1 & PB_0K + N_2^T - N_1 & N_3^T & PB_w + N_4^T & A_0^T & N_1 & \varepsilon PH & E_1^T \\ * & -N_2 - N_2^T & -N_3^T & -N_4^T & (B_0K)^T & N_2 & N_2 & (E_2K)^T \\ * & * & -Q & 0 & 0 & N_3 & 0 & 0 \\ * & * & * & -\gamma_0^2 I & B_w^T & N_4 & 0 & 0 \\ * & * & * & * & -\tau_{\max}^{-1}R^{-1} & 0 & \varepsilon H & 0 \\ * & * & * & * & * & -\tau_{\max}^{-1}R & 0 & 0 \\ * & * & * & * & * & * & -\varepsilon I & 0 \\ * & * & * & * & * & * & 0 & -\varepsilon I \end{bmatrix} < 0, \tag{25}$$

where $\overline{\Pi}_1 = PA_0 + A_0^TP + N_1 + N_1^T + Q + C^TC$.

Proof. Define a Lyapunov–Krasovskii functional as

$$\begin{aligned} V(t) &= V_1(t) + V_2(t) + V_3(t), \\ V_1(t) &= x^T(t)Px(t), \\ V_2(t) &= \int_{t-\tau_{\max}}^{t} x^T(s)Qx(s)ds, \\ V_3(t) &= \int_{-\tau_{\max}}^{0}\int_{t+\theta}^{t} \dot{x}^T(s)R\dot{x}(s)ds\,d\theta, \end{aligned} \tag{26}$$

where P, Q, and R are the symmetric positive definite matrices. Along the trajectory of system (20), the time derivative of $V_i(t)$, $i = 1, 2, 3$, can be computed as follows:

$$\begin{aligned} \dot{V}_1(t) &= x^T(t)\big[P\big((A_0 + \Delta A) + (A_0 + \Delta A)^TP\big)\big]x(t) \\ &\quad + 2x^T(t)P(B_0 + \Delta B)Kx(t-\tau) + 2x^T(t)PB_ww(t), \\ \dot{V}_2(t) &= x^T(t)Qx(t) - x^T(t-\tau_{\max})Qx(t-\tau_{\max}), \\ \dot{V}_3(t) &= \tau_{\max}\dot{x}^T(t)R\dot{x}(t) - \int_{t-\tau_{\max}}^{t} \dot{x}^T(s)R\dot{x}(s)ds. \end{aligned} \tag{27}$$

Define $\xi = \big[x^T(t)\ \ x^T(t-\tau(t))\ \ x^T(t-\tau_{\max})\ \ w^T(t)\big]^T$ and for any matrix $N = \big[N_1^T\ N_2^T\ N_3^T\ N_4^T\big]^T$ with appropriate dimension, we have $\xi^T N(x(t) - x(t-\tau_{\max}) - \int_{t-\tau_{\max}}^{t}\dot{x}(s)ds) = 0$ by using the Newton-Leibniz formula. Thus,

$$\begin{aligned} &-\int_{t-\tau_{\max}}^{t} \dot{x}^T(s)R\dot{x}(s)ds \\ &= -\int_{t-\tau(t)}^{t} \dot{x}^T(s)R\dot{x}(s)ds - 2\xi^T N\int_{t-\tau(t)}^{t}\dot{x}(s)ds \\ &\quad -\tau_{\max}\xi^T NR^{-1}N^T\xi + 2\xi^T N(x(t) - x(t-\tau(t))) \\ &\quad + \tau_{\max}\xi^T NR^{-1}N^T\xi \\ &= -\int_{t-\tau(t)}^{t}\big(\xi^T N + \dot{x}^T R\big)R^{-1}\big(N^T\xi + R\dot{x}\big)ds \\ &\quad + 2\xi^T N(x(t) - x(t-\tau(t))) \\ &\quad + \tau_{\max}\xi^T NR^{-1}N^T\xi. \end{aligned} \tag{28}$$

It is true that

$$-\int_{t-\tau(t)}^{t}\big(\xi^T N + \dot{x}^T R\big)R^{-1}\big(N^T\xi + R\dot{x}\big)ds \leq 0. \tag{29}$$

From (26)–(28), we can obtain

$$\begin{aligned} &\dot{V}(t) + z^T(t)z(t) - \gamma_0^2 w^T(t)w(t) \\ &= x^T(t)\big[P\big((A_0 + \Delta A) + (A_0 + \Delta A)^TP\big)\big]x(t) \\ &\quad + 2x^T(t)P(B_0 + \Delta B)Kx(t-\tau) + 2x^T(t)PB_ww(t) \\ &\quad + x^T(t)Qx(t) - x^T(t-\tau_{\max})Qx(t-\tau_{\max}) \\ &\quad - \int_{t-\tau(t)}^{t}\big(\xi^T N + \dot{x}^T R\big)R^{-1}\big(N^T\xi + R\dot{x}\big)ds \\ &\quad + 2\xi^T N(x(t) - x(t-\tau(t))) + \tau_{\max}\xi^T NR^{-1}N^T\xi \\ &\quad + \tau_{\max}\dot{x}^T(t)R\dot{x}(t) + x^T(t)C^TCx(t) - \gamma_0^2 w^T(t)w(t) \\ &\leq x^T(t)\big[P\big((A_0 + \Delta A) + (A_0 + \Delta A)^TP\big) + Q + C^TC\big]x(t) \\ &\quad + 2x^T(t)P(B_0 + \Delta B)Kx(t-\tau) + 2x^T(t)PB_ww(t) \\ &\quad - x^T(t-\tau_{\max})Qx(t-\tau_{\max}) + \tau_{\max}\dot{x}^T(t)R\dot{x}(t) \\ &\quad + 2\xi^T N[I\ 0\ -I\ 0]\xi + \tau_{\max}\xi^T NR^{-1}N^T\xi \\ &\quad - \gamma_0^2 w^T(t)w(t) \\ &= \xi^T\Phi_1\xi, \end{aligned} \tag{30}$$

where

$$\Phi_1 = \Omega_1 + \Xi_1 + \Xi_1^T + \tau_{\max}NR^{-1}N^T + \tau_{\max}\Xi_2^T R\Xi_2,$$

$$\Omega_1 = \begin{bmatrix} \Pi_1 & P(B_0 + \Delta B)K & 0 & PB_w \\ * & 0 & 0 & 0 \\ * & * & -Q & 0 \\ * & * & * & -\gamma_0^2 I \end{bmatrix}, \tag{31}$$

$$\Pi_1 = P(A_0 + \Delta A) + (A_0 + \Delta A)^TP + Q + C^TC,$$

$$\Xi_1 = N[I\ 0\ -I\ 0],$$

$$\Xi_2 = [A_0 + \Delta A\ \ (B_0 + \Delta B)K\ \ 0\ \ B_w].$$

By the Schur complement, $\Phi_1 < 0$ guarantees that

$$\Phi_2 = \begin{bmatrix} \Omega_2 & \Xi_2^T & N \\ * & -\tau_{\max}^{-1}R^{-1} & 0 \\ * & * & -\tau_{\max}^{-1}R \end{bmatrix} < 0, \tag{32}$$

where

$$\Omega_2 = \begin{bmatrix} \Pi_1 + N_1 + N_1^T & P(B_0 + \Delta B)K - N_1 + N_2^T & N_3^T & PB_w + N_4^T \\ * & -N_2 - N_2^T & -N_3^T & -N_4^T \\ * & * & -Q & 0 \\ * & * & * & -\gamma_0^2 I \end{bmatrix}. \tag{33}$$

To take the parameter uncertainty into consideration, rewrite (32) in the form of (22) as follows:

$$\Phi_2 = \begin{bmatrix} \overline{\Pi}_1 & PB_0K + N_2^T - N_1 & N_3^T & PB_w + N_4^T & A_0^T & N_1 \\ * & -N_2 - N_2^T & -N_3^T & -N_4^T & (B_0K)^T & N_2 \\ * & * & -Q & 0 & 0 & N_3 \\ * & * & * & -\gamma_0^2 I & B_w^T & N_4 \\ * & * & * & * & -\tau_{max}^{-1}R^{-1} & 0 \\ * & * & * & * & * & -\tau_{max}^{-1}R \end{bmatrix}$$

$$+ sys\left\{ \begin{bmatrix} PH \\ 0 \\ 0 \\ 0 \\ H \\ 0 \end{bmatrix} \Lambda \begin{bmatrix} E_1 & E_2K & 0 & 0 & 0 & 0 \end{bmatrix} \right\} < 0, \tag{34}$$

where $\overline{\Pi}_1 = PA_0 + A_0^T P + N_1 + N_1^T + Q + C^T C$ and $sys\{Z\}$ stands for $Z + Z^T$. According to Lemma 1, $\Phi_2 < 0$ holds if and only if there exists a positive scalar $\varepsilon > 0$ such that

$$\begin{bmatrix} \overline{\Pi}_1 & PB_0K + N_2^T - N_1 & N_3^T & PB_w + N_4^T & A_0^T & N_1 \\ * & -N_2 - N_2^T & -N_3^T & -N_4^T & (B_0K)^T & N_2 \\ * & * & -Q & 0 & 0 & N_3 \\ * & * & * & -\gamma_0^2 I & B_w^T & N_4 \\ * & * & * & * & -\tau_{max}^{-1}R^{-1} & 0 \\ * & * & * & * & * & -\tau_{max}^{-1}R \end{bmatrix}$$

$$+ \varepsilon \begin{bmatrix} PH \\ 0 \\ 0 \\ 0 \\ H \\ 0 \end{bmatrix} \begin{bmatrix} (PH)^T & 0 & 0 & 0 & H^T & 0 \end{bmatrix}$$

$$+ \varepsilon^{-1} \begin{bmatrix} E_1^T \\ (E_2K)^T \\ 0 \\ 0 \\ 0 \\ 0 \end{bmatrix} \begin{bmatrix} E_1 & E_2K & 0 & 0 & 0 & 0 \end{bmatrix} < 0. \tag{35}$$

Then, by using a Schur complement operation, equation (25) can be obtained, and the proof is completed. □

It is noted that the matrix inequalities in Theorem 1 are not in the form of LMIs, and in the following, an LMI condition for the existence of desired state-feedback controller will be presented. Thus, the problem of robust H_∞ path-tracking control for network-based vehicle systems will be solved.

Theorem 2. *Given positive constants γ_0 and τ_{max}, there exists a robust H_∞ state-feedback controller in the form of (19) such that closed-loop system (20) is asymptotically stable with an H_∞ disturbance attention level γ_0 if there exist matrices $X > 0$, $\overline{Q} > 0$, $\overline{R} > 0$, general matrices Y, $\overline{N}_i$, $i = 1, \ldots, 4$, and a scalar $\varepsilon > 0$ satisfying*

$$\begin{bmatrix} \Xi_{11} & \Xi_{12} & \Xi_{13} & \Xi_{14} & \Xi_{15} & \Xi_{16} & \Xi_{17} & \Xi_{18} & \Xi_{19} \\ * & \Xi_{22} & \Xi_{23} & \Xi_{24} & \Xi_{25} & \Xi_{26} & 0 & \Xi_{28} & 0 \\ * & * & \Xi_{33} & 0 & 0 & \Xi_{36} & 0 & 0 & 0 \\ * & * & * & \Xi_{44} & \Xi_{45} & \Xi_{46} & 0 & 0 & 0 \\ * & * & * & * & \Xi_{55} & 0 & \Xi_{57} & 0 & 0 \\ * & * & * & * & * & \Xi_{66} & 0 & 0 & 0 \\ * & * & * & * & * & * & \Xi_{77} & 0 & 0 \\ * & * & * & * & * & * & * & \Xi_{88} & 0 \\ * & * & * & * & * & * & * & * & \Xi_{99} \end{bmatrix} < 0, \tag{36}$$

where

$$\Xi_{11} = A_0 X + X A_0^T + \overline{Q} + \overline{N}_1 + \overline{N}_1^T,$$

$$\Xi_{12} = B_0 Y + \overline{N}_2^T - \overline{N}_1,$$

$$\Xi_{13} = \overline{N}_3^T,$$

$$\Xi_{14} = B_w + \overline{N}_4^T,$$

$$\Xi_{15} = X A_0^T,$$

$$\Xi_{16} = \overline{N}_1,$$

$$\Xi_{17} = \varepsilon H,$$

$$\Xi_{18} = X E_1^T,$$

$$\Xi_{19} = X C^T,$$

$$\Xi_{22} = -\overline{N}_2 - \overline{N}_2^T,$$

$$\Xi_{23} = -\overline{N}_3^T,$$

$$\Xi_{24} = -\overline{N}_4^T,$$

$$\Xi_{25} = \left(B_0 Y \right)^T, \qquad (37)$$

$$\Xi_{26} = \overline{N}_2,$$

$$\Xi_{28} = \left(E_2 Y \right)^T,$$

$$\Xi_{33} = -\overline{Q},$$

$$\Xi_{36} = \overline{N}_3,$$

$$\Xi_{44} = -\gamma_0^2 I,$$

$$\Xi_{45} = B_w^T$$

$$\Xi_{46} = \overline{N}_4,$$

$$\Xi_{55} = -\tau_{\max}^{-1} \overline{R},$$

$$\Xi_{57} = \varepsilon H,$$

$$\Xi_{66} = \tau_{\max}^{-1} \left(\overline{R} - 2X \right),$$

$$\Xi_{77} = -\varepsilon I,$$

$$\Xi_{88} = -\varepsilon I,$$

$$\Xi_{99} = -I.$$

Moreover, the control gain matrix is given by $K = Y X^{-1}$.

Proof. From Theorem 1, it is known that there exists a state-feedback controller in the form of (19) such that closed-loop system (20) is asymptotically stable with an H_∞ disturbance attention level γ_0 if there exist matrices $P > 0$, $Q > 0$, $R > 0$, general matrices N_i, $i = 1, \ldots, 4$, and scalars $\varepsilon > 0$ satisfying (25). Performing a congruence transformation to (25) by diag$\{P^{-1}, P^{-1}, P^{-1}, I, I, P^{-1}, I, I\}$, it follows that

$$\begin{bmatrix} \Theta_{11} & \Theta_{12} & \Theta_{13} & \Theta_{14} & \Theta_{15} & \Theta_{16} & \Theta_{17} & \Theta_{18} \\ * & \Theta_{22} & \Theta_{23} & \Theta_{24} & \Theta_{25} & \Theta_{26} & 0 & \Theta_{28} \\ * & * & \Theta_{33} & 0 & 0 & \Theta_{36} & 0 & 0 \\ * & * & * & \Theta_{44} & \Theta_{45} & \Theta_{46} & 0 & 0 \\ * & * & * & * & \Theta_{55} & 0 & \Theta_{57} & 0 \\ * & * & * & * & * & \Theta_{66} & 0 & 0 \\ * & * & * & * & * & * & \Theta_{77} & 0 \\ * & * & * & * & * & * & * & \Theta_{88} \end{bmatrix} < 0, \qquad (38)$$

where

$$\Theta_{11} = A_0 P^{-1} + P^{-1} A_0^T + P^{-1} N_1 P^{-1} + P^{-1} N_1^T P^{-1}$$
$$\qquad + P^{-1} Q P^{-1} + P^{-1} C^T C P^{-1},$$

$$\Theta_{12} = B_0 K P^{-1} + P^{-1} N_2^T P^{-1} - P^{-1} N_1 P^{-1},$$

$$\Theta_{13} = P^{-1} N_3^T P^{-1},$$

$$\Theta_{14} = B_w + P^{-1} N_4^T,$$

$$\Theta_{15} = P^{-1} A_0^T,$$

$$\Theta_{16} = P^{-1} N_1 P^{-1},$$

$$\Theta_{17} = \varepsilon H,$$

$$\Theta_{18} = P^{-1} E_1^T,$$

$$\Theta_{22} = -P^{-1} N_2 P^{-1} - P^{-1} N_2^T P^{-1},$$

$$\Theta_{23} = -P^{-1} N_3^T P^{-1},$$

$$\Theta_{24} = -P^{-1} N_4^T,$$

$$\Theta_{25} = P^{-1} K^T B_0^T, \qquad (39)$$

$$\Theta_{26} = P^{-1} N_2 P^{-1},$$

$$\Theta_{28} = P^{-1} K^T E_2^T,$$

$$\Theta_{33} = -P^{-1} Q P^{-1},$$

$$\Theta_{36} = P^{-1} N_3 P^{-1},$$

$$\Theta_{44} = -\gamma_0^2 I,$$

$$\Theta_{45} = B_w^T,$$

$$\Theta_{46} = N_4 P^{-1},$$

$$\Theta_{55} = -\tau_{\max}^{-1} R^{-1},$$

$$\Theta_{57} = \varepsilon H,$$

$$\Theta_{66} = -\tau_{\max}^{-1} P^{-1} R P^{-1},$$

$$\Theta_{77} = -\varepsilon I,$$

$$\Theta_{88} = -\varepsilon I.$$

Due to the existence of the nonlinear term $-\tau_{\max}^{-1} P^{-1} R P^{-1}$, the above inequality cannot be solved by the standard numerical software. Note that $R > 0$, it follows that $(R^{-1} - P^{-1}) R (R^{-1} - P^{-1}) \geq 0$, which is equivalent to $-\tau_{\max}^{-1} P^{-1} R P^{-1} \leq \tau_{\max}^{-1} (R^{-1} - 2P^{-1})$ by Lemma 2. Define the following matrix variables:

$$X = P^{-1},$$

$$Y = KP^{-1},$$

$$\overline{Q} = P^{-1}QP^{-1},$$

$$\overline{R} = R^{-1},$$

$$\overline{N}_1 = P^{-1}N_1P^{-1},$$

$$\overline{N}_2 = P^{-1}N_2P^{-1},$$

$$\overline{N}_3 = P^{-1}N_3P^{-1},$$

$$\overline{N}_4 = N_4P^{-1},$$

$$(40)$$

and perform a Schur complement operation to the term XC^TCX in the (1, 1) block. Equation (36) can be obtained, and this completes the proof of Theorem 2. □

Remark 1. It is noted that (36) is an LMI not only over the matrix variables but also over the scalar γ_0. Thus, for the optimization variable γ_0, the minimum H_∞ disturbance attention level bound can be obtained with the proposed controller in terms of the feasibility of (36). This means to solve the following convex optimization problem: minimize γ_0 subject to inequality (36) over matrices $X > 0, \overline{Q} > 0, \overline{R} > 0$, general matrices Y, $\overline{N}_i$, $i = 1, \ldots, 4$, and scalar $\varepsilon > 0$.

When there are no delay and packet dropout in the signal transmission, the vehicle path-tracking model in (20) reads

$$\dot{x}(t) = (A_0 + \Delta A)x(t) + (B_0 + \Delta B)u(t) + B_w w(t). \quad (41)$$

The state-feedback controller is expressed as

$$u(t) = K_{zd}x(t), \quad (42)$$

where K_{zd} is the control gain to be designed. And the closed-loop system can be written as

$$\dot{x}(t) = [(A_0 + \Delta A) + (B_0 + \Delta B)K_{zd}]x(t) + B_w w(t),$$
$$z(t) = Cx(t). \quad (43)$$

Then, following the similar lines as in the proof of Theorem 2, the following corollary can be obtained.

Corollary 1. *Given a positive constant γ_0, there exists a robust H_∞ state-feedback controller in the form of (42) such that closed-loop system (43) is asymptotically stable with an H_∞ disturbance attention level γ_0 if there exist matrix $\overline{P} > 0$, general matrix $\overline{X}$, and a scalar $\varepsilon_0 > 0$ satisfying*

$$\begin{bmatrix} \overline{\Xi}_1 & B_w & \varepsilon_0 H & \overline{P}E_1^T + \overline{X}^T E_2^T & \overline{P}C^T \\ * & -\gamma_0^2 I & 0 & 0 & 0 \\ * & * & -\varepsilon_0 I & 0 & 0 \\ * & * & * & -\varepsilon_0 I & 0 \\ * & * & * & * & -I \end{bmatrix} < 0, \quad (44)$$

where $\overline{\Xi}_1 = A_0\overline{P} + B_0\overline{X} + \overline{P}A_0^T + (B_0\overline{X})^T$ and the control gain is given by $K_{zd} = \overline{X}\,\overline{P}^{-1}$.
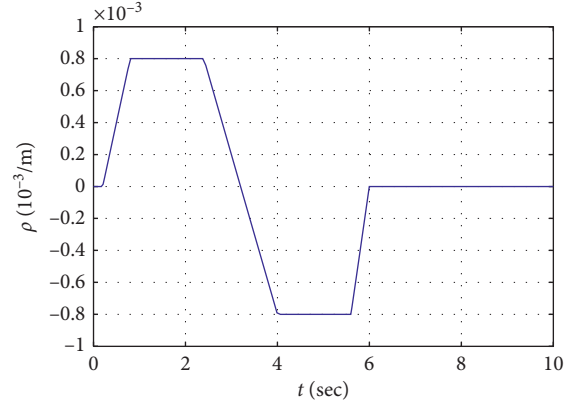
FIGURE 4: Road curvature of the single-lane change maneuver.

--- DC ($\tau = 0.04$ s)

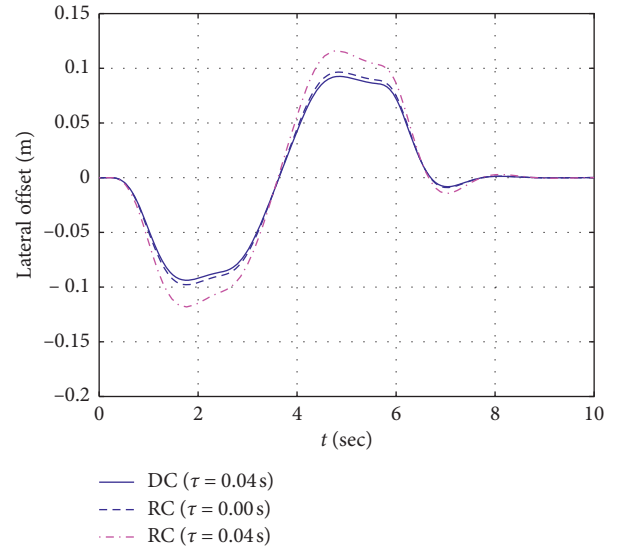- - - RC ($\tau = 0.00$ s)

-·-· RC ($\tau = 0.04$ s)

FIGURE 5: Lateral offset results of the single-lane change maneuver.

4. Simulation Results

In this section, two simulation manoeuvers are presented to examine the effectiveness of the proposed method. The data of the vehicle system are listed as follows: $m = 1500$ kg, $I_z = 2500$ kgm^2, $l_f = 1.3$ m, $l_r = 1.4$ m, $l_s = 0.8$ m, $C_f = 40{,}000$ Nm/rad, and $C_r = 40{,}000$ Nm/rad. Suppose the parameter uncertainty of the cornering stiffness is 20% of its nominal value. The maximum value of the measurement and transmission delay is assumed to be 30 ms. The maximum number of packet dropout is 5, and the sampling period is 2 ms; then, the maximum delay is 40 ms. The obtained minimum H_∞ performance index in terms of the feasibility of (36) is 0.6256. For the sake of convenience, the proposed robust H_∞ controller is named as DC, and the robust controller without delay and packet dropout is denoted as RC.

In the first simulation, the vehicle is assumed to finish a single-lane change maneuver. The vehicle velocity is set as 20 (m/s), and the initial lateral displacement is 0 m. The road curvature is shown in Figure 4, and it can be seen that in this
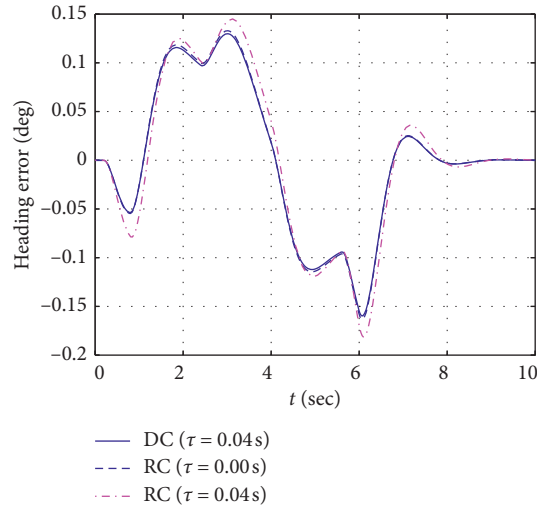
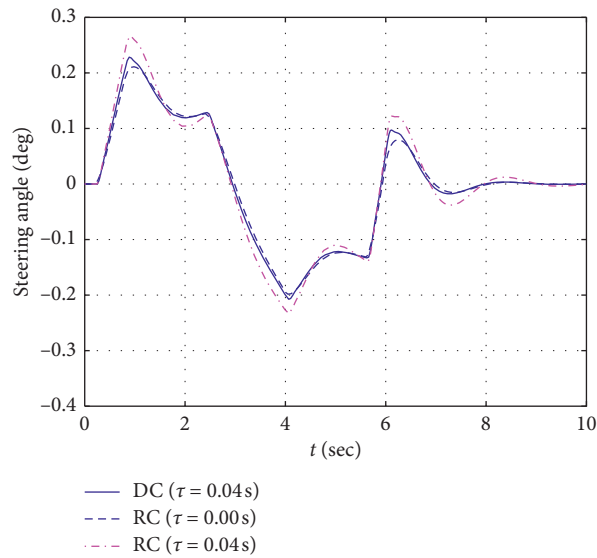Figure 6: Heading error results of the single-lane change maneuver.

Figure 7: Control inputs of the single-lane change maneuver.

case the road curvature varies smoothly. The simulation results for the lateral offset in the single-lane change maneuver are presented in Figure 5. It can be observed that with the same time-delay $\tau = 0.04$ s, the lateral offset of the vehicle by DC is smaller than that of RC ($\tau = 0.04$ s) and better than that of RC ($\tau = 0.00$ s). The heading errors for both controllers are compared in Figure 6; it is shown that the DC yields more smooth responses for vehicle orientation control, while RC ($\tau = 0.04$ s) causes much larger overshoot. The delay and packet dropout cause large oscillations in the path-tracking states and deteriorate the performance of RC. The front-wheel steering angle is plotted in Figure 7, and it shows a similar variation trend to the road curvature and is controlled in reasonable regions with several fluctuations. The global trajectory results are shown in Figure 8; it can be seen that the vehicle tracks the desired path more accurately with the proposed robust controller than RC in presence of delay and packet dropout, parameter uncertainties, and external disturbances.

In the second simulation, a double-lane change maneuver is chosen to simulate the severe driving conditions. The initial velocity is 20 (m/s), and the road curvature is plotted in Figure 9, where some step variations are included in the road curvature. The simulation results for the lateral offset and heading error in the double-lane change maneuver are shown in Figures 10 and 11. It can be seen that even with some step variations introduced in the road curvature, there are less number of oscillations of the path-tracking errors by using DC than RC ($\tau = 0.04$ s), considering delay and packet dropout. Figure 12 shows that the path-tracking control effect of steering input of DC ($\tau = 0.04$ s) is good as that of RC ($\tau = 0.00$ s). The global trajectory results are presented in Figure 13, and it can be observed that the path-tracking task is finished better by the
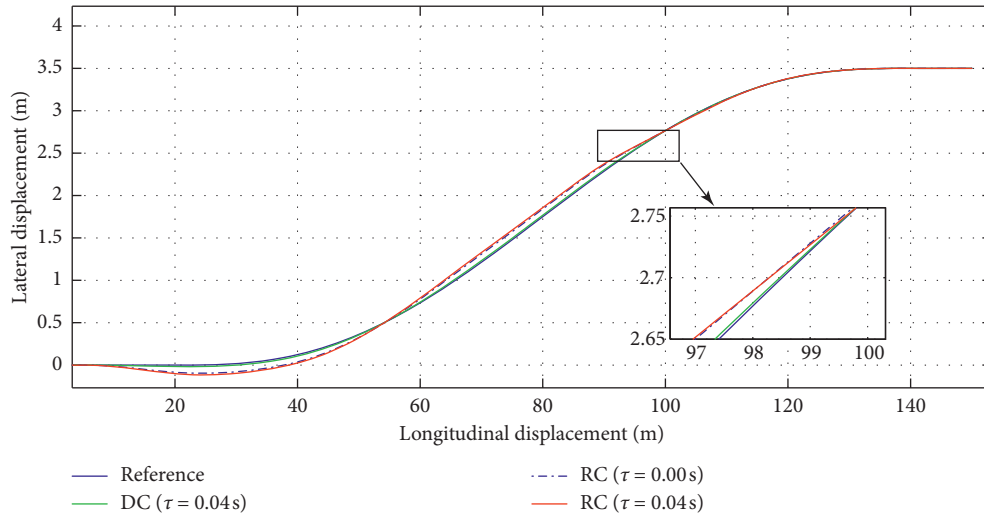
Figure 8: Global trajectory results of the single-lane change maneuver.
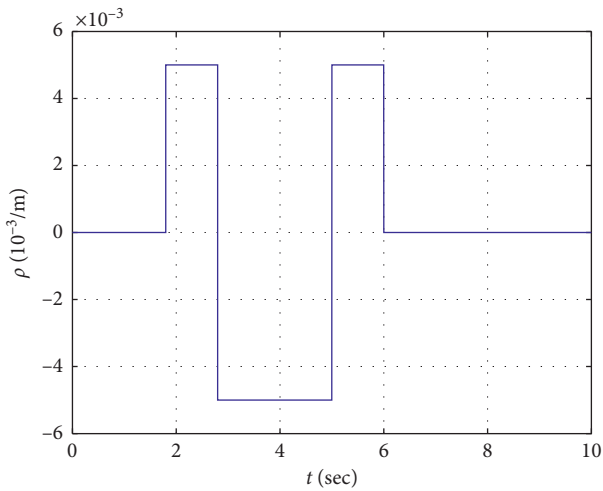

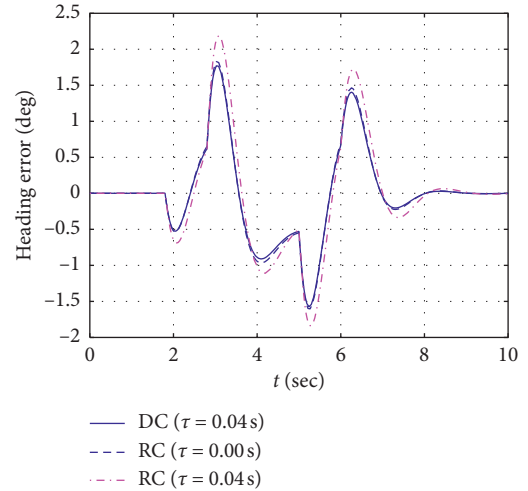Figure 9: Road curvature of the double-lane change maneuver.

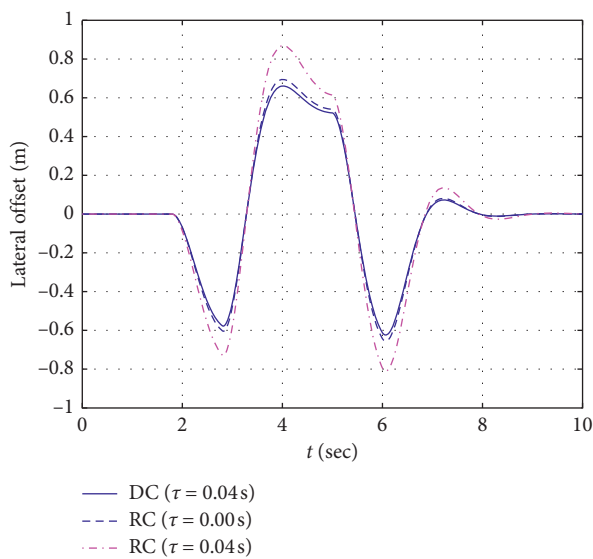Figure 11: Heading error results of the double-change maneuver.

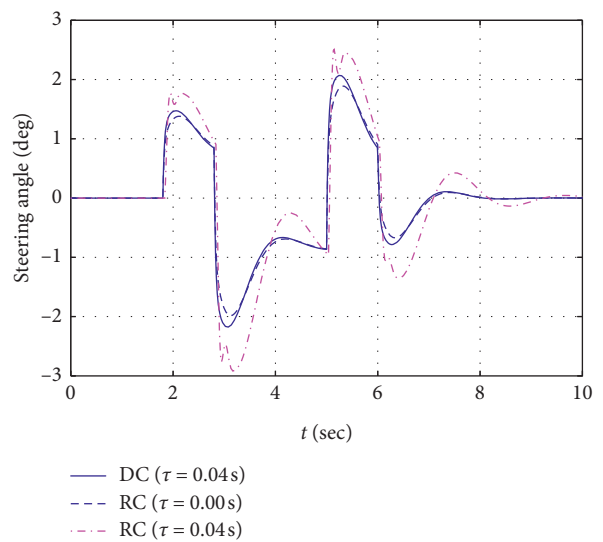Figure 10: Lateral offset results of the double-change maneuver.

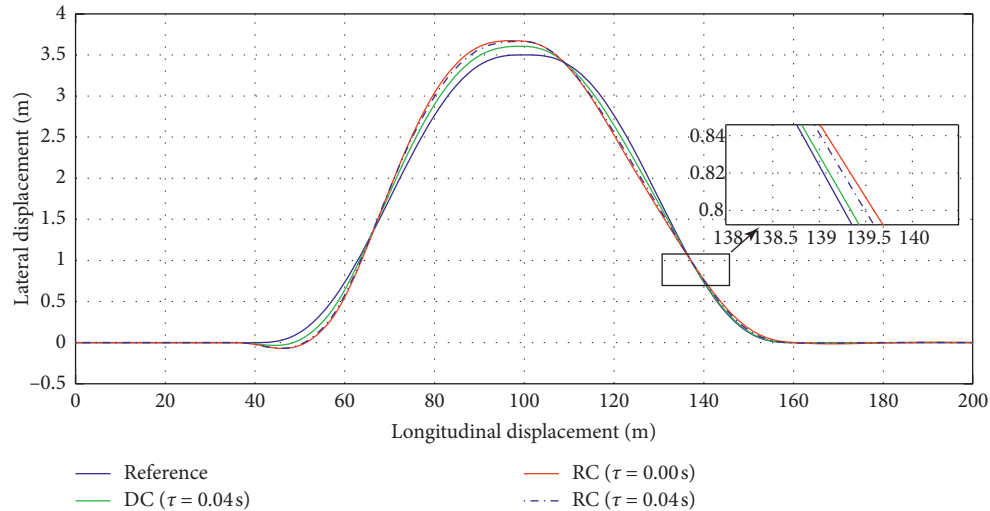Figure 12: Control inputs of the double-lane change maneuver.

Figure 13: Global trajectory results of the double-lane change maneuver.

controller DC than the controller RC. Thus, the vehicle can be well controlled even on the tough driving conditions, and this justifies the effectiveness and robustness of the proposed controller.

5. Conclusions

In the paper, a robust H_∞ controller is proposed to control network-based autonomous vehicles to track the desired path in presence of time-delay and packet dropout. The yaw rate and sideslip angle are also regulated to improve the vehicle lateral stability. The closed-loop path-tracking control system is asymptotically stable with the predefined H_∞ disturbance attention performance if certain LMIs conditions are satisfied. The proposed controller is robust to the parameter uncertainties and external disturbances. Furthermore, the superiority of the proposed control scheme can be validated by comparison with no delay and packet dropout case. Simulation results under different manoeuvres are presented to illustrate the effectiveness of the control scheme. The analysis on how to further reduce the conservatism of the obtained result is considered to be topics of our future work.

Data Availability

The data used to support the findings of this study are included within the article.

Conflicts of Interest

The authors declare that there are no conflicts of interest regarding the publication of this paper.

Acknowledgments

References

[1] J. M. Anderson, *Autonomous Vehicle Technology: A Guide for Policymakers*, Rand Corporation, Santa Monica, CA, USA, 2014.

[2] R. Potluri and A. K. Singh, "Path-tracking control of an autonomous 4WS4WD electric vehicle using its natural feedback loops," *IEEE Transactions on Control Systems Technology*, vol. 23, no. 5, pp. 2053–2062, 2015.

[3] Q. Zhang, L. Lapierre, and X. Xiang, "Distributed control of coordinated path tracking for networked nonholonomic mobile vehicles," *IEEE Transactions on Industrial Informatics*, vol. 9, no. 1, pp. 472–484, 2013.

[4] J. Ni, J. Hu, and C. Xiang, "Robust control in diagonal move steer mode and experiment on an X-by-Wire UGV," *IEEE/ASME Transactions on Mechatronics*, vol. 24, no. 2, pp. 572–584, 2019.

[5] C. Chen, Y. Jia, J. Du, and F. Yu, "Lane keeping control for autonomous 4WS4WD vehicles subject to wheel slip constraint," in *Proceedings of the American Control Conference*, pp. 6515–6520, Montral, Canada, June 2012.

[6] T. Faulwasser and R. Findeisen, "Nonlinear model predictive control for constrained output path following," *IEEE Transactions on Automatic Control*, vol. 61, no. 4, pp. 1026–1039, 2016.

[7] B. Gutjahr, L. Gröll, and M. Werling, "Lateral vehicle trajectory optimization using constrained linear time-varying MPC," *IEEE Transactions on Intelligent Transportation Systems*, vol. 18, no. 6, pp. 1586–1595, 2017.

[8] L. Guo, P.-S. Ge, M. Yue, and Y.-B. Zhao, "Lane changing trajectory planning and tracking controller design for intelligent vehicle running on curved road," *Mathematical Problems in Engineering*, vol. 2014, Article ID 478573, 9 pages, 2014.

[9] C. Hu, R. Wang, F. Yan, and N. Chen, "Output constraint control on path following of four-wheel independently actuated autonomous ground vehicles," *IEEE Transactions on Vehicular Technology*, vol. 65, no. 6, pp. 4033–4043, 2016.

[10] C. Chen, M. Shu, and R. Liu, "Virtual-point-based asymptotic tracking control of 4 ws vehicles," *International Journal of Control, Automation and Systems*, vol. 13, no. 2, pp. 371–378, 2015.

[11] R. Wang, H. Zhang, and J. Wang, "Linear parameter-varying controller design for four-wheel independently actuated electric ground vehicles with active steering systems," *IEEE Transactions on Control Systems Technology*, vol. 22, no. 4, pp. 1281–1296, 2014.

[12] X. J. Jin, G. Yin, and N. Chen, "Gain-scheduled robust control for lateral stability of four-wheel-independent-drive electric vehicles via linear parameter-varying technique," *Mechatronics*, vol. 30, pp. 286–296, 2015.

[13] S. E. Li, F. Gao, K. Li, L.-Y. Wang, K. You, and D. Cao, "Robust longitudinal control of multi-vehicle systems-a distributed H-infinity method," *IEEE Transactions on Intelligent Transportation Systems*, vol. 19, no. 9, pp. 2779–2788, 2018.

[14] C. Chen, Y. Jia, M. Shu, and Y. Wang, "Hierarchical adaptive path-tracking control for autonomous vehicles," *IEEE Transactions on Intelligent Transportation Systems*, vol. 16, no. 5, pp. 2900–2912, 2015.

[15] A. P. Aguiar and J. P. Hespanha, "Trajectory-tracking and path-following of underactuated autonomous vehicles with parametric modeling uncertainty," *IEEE Transactions on Automatic Control*, vol. 52, no. 8, pp. 1362–1379, 2007.

[16] R. Wang, C. Hu, F. Yan, and M. Chadli, "Composite nonlinear feedback control for path following of four-wheel independently actuated autonomous ground vehicles," *IEEE Transactions on Intelligent Transportation Systems*, vol. 17, no. 7, pp. 2063–2074, 2016.

[17] L. Zhang, H. Gao, and O. Kaynak, "Network-induced constraints in networked control systems-a survey," *IEEE Transactions on Industrial Informatics*, vol. 9, no. 1, pp. 403–416, 2013.

[18] X. Zhu, H. Zhang, J. Wang, and Z. Fang, "Robust lateral motion control of electric ground vehicles with random network-induced delays," *IEEE Transactions on Vehicular Technology*, vol. 64, no. 11, pp. 4985–4995, 2015.

[19] R. Postoyan, N. van de Wouw, D. Nesic, W. P. M. H. Heemels, and H. Heemels, "Tracking control for nonlinear networked control systems," *IEEE Transactions on Automatic Control*, vol. 59, no. 6, pp. 1539–1554, 2014.

[20] H. Gao, T. Chen, and J. Lam, "A new delay system approach to network-based control," *Automatica*, vol. 44, no. 1, pp. 39–52, 2008.

[21] J. Zhou and D. Zhang, "H-Infinity fault detection for delta operator systems with random two-channels packet losses and limited communication," *IEEE Access*, vol. 7, pp. 94448–94459, 2019.

[22] Y. Wang, G. Song, J. Zhao, J. Sun, and G. Zhuang, "Reliable mixed H_∞ and passive control for networked control systems under adaptive event-triggered scheme with actuator faults and randomly occurring nonlinear perturbations," *ISA Transactions*, vol. 89, pp. 45–57, 2019.

[23] Y. Wang, G. Zhuang, and F. Chen, "A dynamic event-triggered H_∞ control for singular Markov jump systems with redundant channels," *International Journal of Systems Science*, vol. 51, no. 1, pp. 158–179, 2020.

[24] Y. Wang, G. Zhuang, and F. Chen, "Event-based asynchronous dissipative filtering for T-S fuzzy singular Markovian jump systems with redundant channels," *Nonlinear Analysis: Hybrid Systems*, vol. 34, pp. 264–283, 2019.

[25] X.-S. Zhan, Z.-H. Guan, X.-H. Zhang, and F.-S. Yuan, "Optimal tracking performance and design of networked control systems with packet dropouts," *Journal of the Franklin Institute*, vol. 350, no. 10, pp. 3205–3216, 2013.

[26] X.-S. Zhan, J. Wu, T. Jiang, and X.-W. Jiang, "Optimal performance of networked control systems under the packet dropouts and channel noise," *ISA Transactions*, vol. 58, no. 5, pp. 214–221, 2015.

[27] X.-S. Zhan, L.-L. Cheng, J. Wu, and H.-C. Yan, "Modified tracking performance limitation of networked time-delay systems with two-channel constraints," *Journal of the Franklin Institute*, vol. 356, no. 12, pp. 6401–6418, 2019.

[28] R. Wang, Q. Sun, D. Ma, and Z. Liu, "The small-signal stability analysis of the droop-controlled converter in electromagnetic timescale," *IEEE Transactions on Sustainable Energy*, vol. 10, no. 3, pp. 1459–1469, 2019.

[29] Y. Li, H. Zhang, X. Liang, and B. Huang, "Event-triggered-based distributed cooperative energy management for multienergy systems," *IEEE Transactions on Industrial Informatics*, vol. 15, no. 4, pp. 2008–2022, 2019.

[30] H. Zhang, Y. Li, D. W. Gao, and J. Zhou, "Distributed optimal energy management for energy internet," *IEEE Transactions on Industrial Informatics*, vol. 13, no. 6, pp. 3081–3097, 2017.

[31] Y. Li, H. Zhang, B. Huang, and J. Han, "A distributed Newton-Raphson-based coordination algorithm for multi-agent optimization with discrete-time communication," *Neural Computing and Applications*, 2018.

[32] G. Phanomchoeng, R. Rajamani, and D. Piyabongkarn, "Nonlinear observer for bounded jacobian systems, with applications to automotive slip angle estimation," *IEEE Transactions on Automatic Control*, vol. 56, no. 5, pp. 1163–1170, 2011.